

REFLECTED SPECTRA PREDICTIONS FOR CHIRPED FIBRE BRAGG GRATINGS USED FOR DISBOND DETECTION IN COMPOSITE/COMPOSITE JOINTS

Palaniappan J¹, Ogin S L¹, Capell T F¹, Thorne A M¹, Reed G T², A D Crocombe¹, Tjin S C³ and Mohanty L³

¹School of Engineering, University of Surrey, GU2 7XH, UK

²School of Electronics and Physical Sciences, University of Surrey, GU2 7XH, UK

³School of Electrical and Electronic Engineering, Photonics Research Centre, Nanyang Technological University, Singapore

Keywords: *Adhesively bonded joints, disbond, chirped fibre Bragg grating*

Abstract

In this paper it is shown that a chirped fibre Bragg grating sensor embedded within a composite adherend can be used to monitor disbond initiation and propagation in an adhesively bonded single lap-joint. Characteristic changes in the reflected spectra from the sensor indicate both disbond initiation and the current position of the disbond front to within about 2 mm (a distance which depends on adherend material and sensor position in relation to the adhesive bondline). When the sensor extends the full overlap length, disbond initiation from either end of the overlap can be monitored. The results have been modelled using a combination of finite-element analysis and commercial software for predicting FBG spectra; the predicted spectra are in very good agreement with experiment. The CFBG sensor technique could provide the basis for monitoring a wide range of bonded joints and structures where one adherend is a composite material.

1 Introduction

Joining of composites through adhesive bonding is an attractive alternative to mechanical fasteners because both similar and dissimilar materials can be joined with a uniform stress distribution over the bonded area. However, the difficulty with bonded constructions is, of course, that they cannot be disassembled easily and that structural health monitoring of joint integrity, both immediately after fabrication and during service,

remains a major concern. A number of NDE (non-destructive evaluation) techniques have been suggested to monitor bonded joints based on ultrasonic [1], acoustic [2], thermal [3] and backface strain measurements [4], together with a range of fibre optical techniques. Among the optical techniques, the use of uniform fibre Bragg grating (FBG) sensors has been the most widely chosen method, with a number of such demonstrations available in the literature for monitoring bonded joints, repairs and structures [5-10]. In addition to uniform fibre Bragg gratings, chirped fibre Bragg grating (CFBG) sensors have more recently been investigated for damage monitoring in composites and bonded joints (e.g. [11-16]), following the pioneering use of this type of sensor for monitoring composite damage by Takeda, Okabe and colleagues [17]. The chirped FBG sensors have a linear variation of the grating period and hence reflect a spectral band of wavelengths with roughly equal intensity. The spectral bandwidth of the reflected spectra corresponds to the physical length of the sensor and this relationship is used to find the location of damage.

In the current paper, previous work [15,16] on locating the position of a disbond in a bonded composite joint with similar adherends is extended to show that disbonding from either end of the joint can be monitored and that the reflected spectra from the CFBG sensor can be predicted for both cases.

2 Materials and methods

2.1 Materials

Transparent GFRP single-lap bonded joints (SLJs), 20 mm wide and 120 mm long, with an overlap length of 60 mm, were fabricated for this study. The adherends were cut from frame-wound, wet lay-up GFRP panels having a lay-up of $(0_2/90/0_6)_s$, where the thickness of each ply was 0.25 mm, giving an overall adherend thickness of 4.5 mm. During fabrication, CFBGs were embedded within one adherend, near the first 0/90 interface, and approximately 0.5 mm from the bond line. The low-wavelength end of the sensor was adjacent to the cut end of the adherend. The CFBGs had a full width at the half maximum of the reflected spectrum of 20 nm, and lengths of 15, 30, 45 and 60 mm (the 60 mm length sensors extend the full length of the overlap of the joint). A one-part elevated temperature cure adhesive (AV 119) was applied to the surface of each adherend and a uniform bondline was ensured using two 0.4 mm diameter wire spacers. The SLJs were cured at 120° C for 1 h in a finger-tightened spring-loaded jig to maintain light pressure on the joint. Further fabrication details can be found in previous papers [15,16]. Figure 1 shows a schematic diagram of the GFRP-GFRP joint with the embedded CFBG; the grating spacing (Δ) within the CFBG sensor increases uniformly from the end of the adherend within which it is embedded.

2.2 Experimental methods

The optical fibre containing the CFBG sensor was spliced to the optical arrangement which consisted of a broadband light source, coupler and optical spectrum analyser (details are provided in [14-16]). The bonded joints were subjected to fatigue loading using a computer-controlled servo-hydraulic fatigue machine (Instron 1341); a peak load of 8 kN was used, an R-value ($R = \sigma_{\min}/\sigma_{\max}$) of 0.1, and a sinusoidal waveform with a frequency of 3 Hz. The glass/epoxy SLJ is transparent, enabling the propagation of the disbond to be monitored visually during the tests and recorded with a camera for direct comparison with the measurements made using the CFBG sensor. The cyclic loading was interrupted at increasing numbers of cycles in order (a) to capture the image using an *in situ* digital camera, and (b) to record the reflected spectrum of the CFBG sensor with the joint subjected to a load of 5 kN.

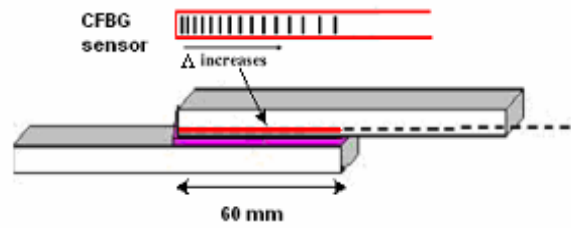


Fig. 1. Schematic of the GFRP-GFRP bonded joint with an embedded CFBG sensor. Note the low wavelength end of the sensor is adjacent to the cut end of the adherend

3 Results and Discussion

3.1 Disbond initiation and growth: low wavelength end of the CFBG sensor

Previous work [15], which used a chirped sensor with a length of 45 mm, showed that disbands initiating at the low wavelength end of the CFBG sensor can be detected. Figure 2 shows the reflected spectra before and after the initiation of a disbond adjacent to the end of a sensor with a length of 15 mm. When a disbond initiates, the end of the adherend adjacent to the disbond is unloaded and hence relaxes, causing the sensor spacing to reduce locally, and hence the low wavelength end of the spectrum moves to lower wavelengths, as shown in figure 2.

Figure 3 shows the overlap length of the transparent GFRP-GFRP bonded joint after 14,000, 15,000 and 17,000 cycles, with the arrows indicating the position of the CFBG sensor in relation to the disbond front position. The progression of the disbond is indicated in the reflection spectrum by a perturbation which, for a 15 mm sensor, appears as a small rise and then fall in the reflected intensity, followed by a more gentle rise (the shape of the perturbation is slightly different from the perturbation seen for a sensor length of 45 mm [15]). Figures 4(a) and 4(b), taken after 14,000 and 15,000 cycles, respectively, show that the perturbation moves to higher wavelengths as the disbond front extends along the bonded joint.

REFLECTED SPECTRA PREDICTIONS FOR CHIRPED FIBRE BRAGG GRATINGS USED FOR DISBOND DETECTION IN COMPOSITE/COMPOSITE JOINTS

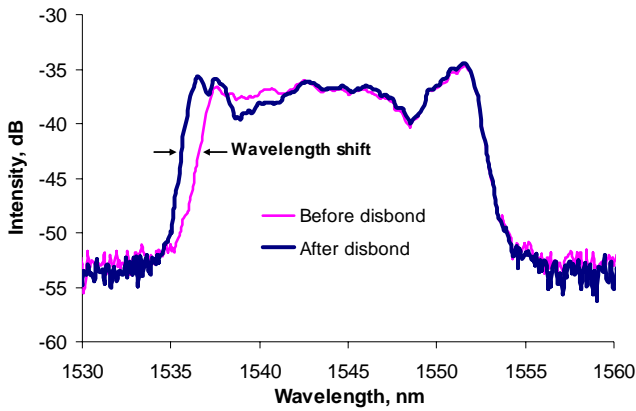


Fig. 2. Reflection spectra recorded before and after disbond using a 15 mm length CFBG sensor and with the joint under a small tensile load. The low-wavelength end of the spectrum shifts to lower wavelengths after the disbond initiates.

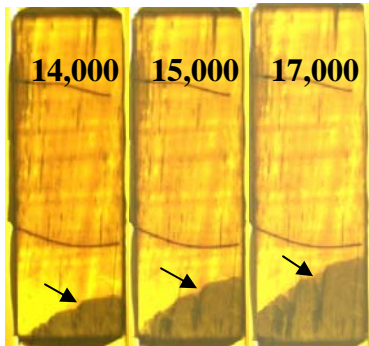


Fig. 3. Images of a GFRP-GFRP bonded joint showing disbond growth with fatigue cycles; the arrows in indicate the position of the CFBG sensor.

In previous work using a CFBG with a sensor length of 45 mm [16], it was shown both experimentally and theoretically that the perturbation in the spectrum which indicates the disbond front position has the form of a local, and reasonably symmetrical, dip in the spectrum. For the sensor with a length of 15 mm but the same spectral bandwidth of 20 nm, the spectrum predicted by a combination of finite-element modeling and OptiGrating software [18] is shown in figure 5 for a disbond length of 5 mm. The short vertical line in the predicted spectrum represents the position of the disbond front, which is about 0.5 mm from the minimum of the perturbation. The shape of the predicted spectrum is in good agreement with the experimental results (figure 4).

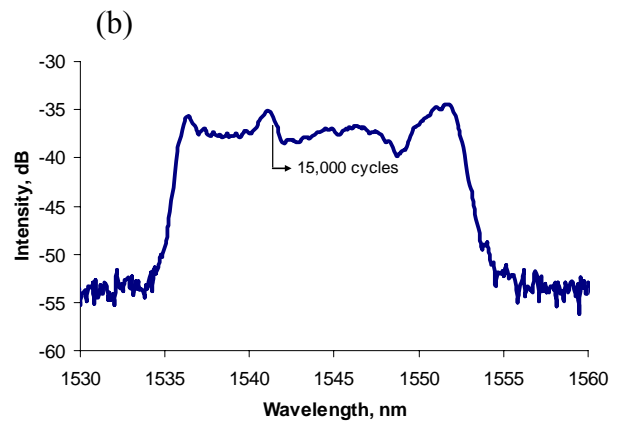
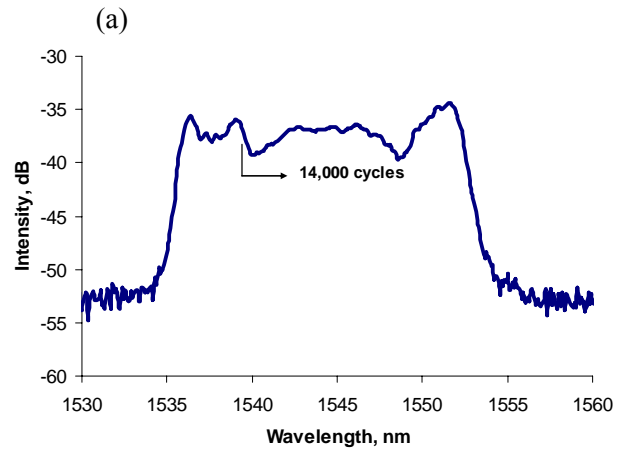


Fig. 4. Reflection spectra recorded at (a) 14000 cycles and (b) 15000 cycles. Perturbation in intensity due to the disbond and the movement of this perturbation as the disbond propagates can be noted.

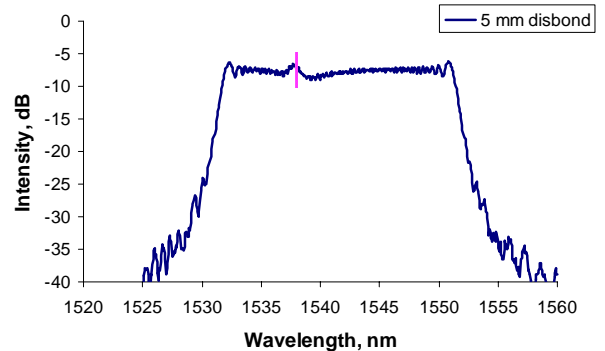


Fig. 5. Predicted reflection spectrum for a 15 mm CFBG sensor with a 5 mm disbond. The small vertical line represents the disbond front position.

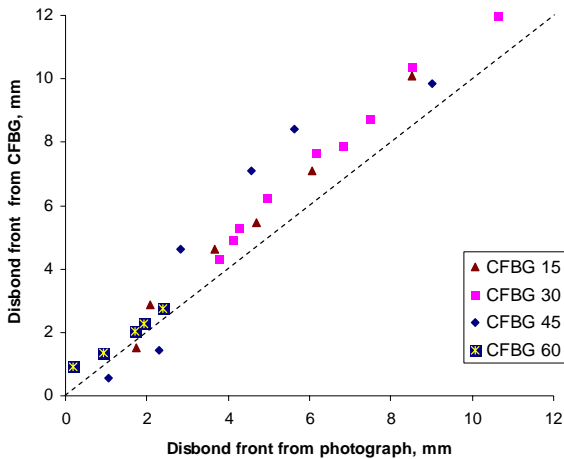


Fig. 6. Comparison of the disbond front position measured from photographs and using the CFBG sensor for sensors with lengths of 15 mm, 30 mm, 45 mm and 60 mm

Figure 6 shows a comparison of photographic and CFBG sensor determinations of the disbond front position in bonded joints for sensor lengths of 15 mm, 30 mm, 45 mm and 60 mm. In all cases, the sensors measure the disbond position to within about 2 mm of the position determined from *in situ* photographs of the transparent bonded joints.

3.2 Disbond initiation and growth: high wavelength end of the CFBG sensor

Of course, a disbond can initiate at either end of a single lap-joint and this section shows that a disbond initiating at the high wavelength end can also be monitored. Figure 7 shows the reflected spectra for a CFBG sensor which extends the full length of a 60 mm bonded joint, both before and after disbond initiation. Figure 7 compares a reflected spectrum before fatigue cycling (hence before any damage development) and after 25,000 fatigue cycles, by which point a disbond had initiated. The fatigue parameters for this experiment were the same as described earlier, and again the spectra were recorded under a load of 5 kN.

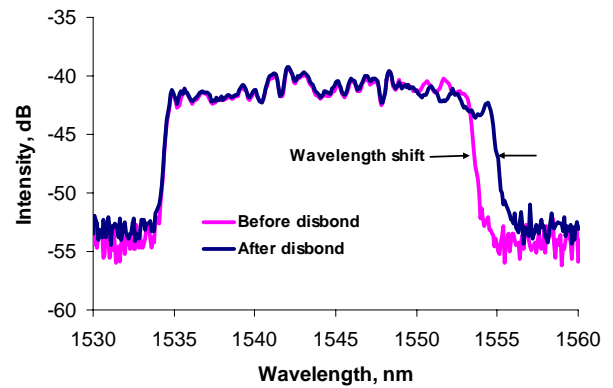


Fig. 7. Comparison of reflection spectra for 60 mm CFBG sensor before and after disbond.

In this case, there is a shift in the high wavelength end of the CFBG reflected spectrum to higher wavelengths as a consequence of disbond initiation, which can be explained as follows. For this configuration, when the SLJ disbonds at the high wavelength end, it unloads one of the GFRP adherends locally, at the position of disbond, but enhances the load locally in the adherend which contains the embedded sensor. The consequence is that this adherend sees an enhanced strain, which leads locally to an increased spacing for the gratings of the CFBG sensor near the sensor end, and hence the reflected spectrum here shifts to higher wavelengths.



Fig. 8. Schematic of GFRP-GFRP bonded joint showing the disbond growth from the higher wavelength end of CFBG at various increasing fatigue cycles.

REFLECTED SPECTRA PREDICTIONS FOR CHIRPED FIBRE BRAGG GRATINGS USED FOR DISBOND DETECTION IN COMPOSITE/COMPOSITE JOINTS

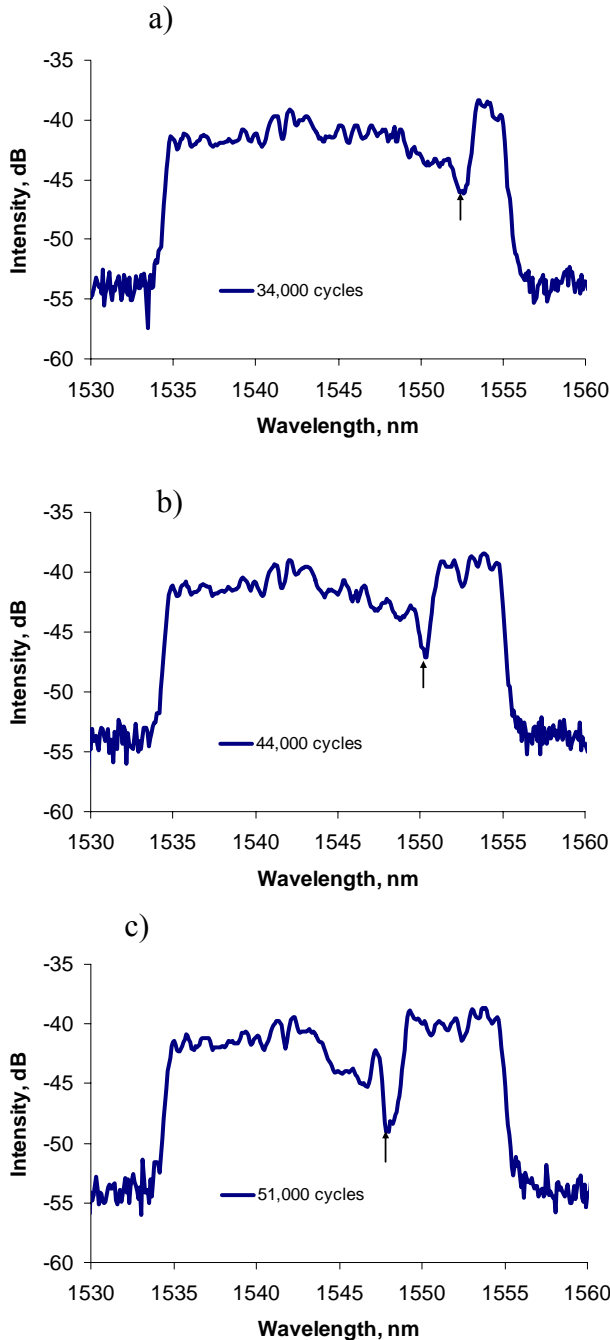


Fig. 9. CFBG reflection spectra, taken with the joint under a small load after (a) 34,000 cycles, (b) 44,000 cycles and (c) 51,000 cycles.

The propagation of the disbond with continued fatigue cycling is shown in figure 8, and corresponding reflected spectra, taken with the fatigue loading interrupted, are shown in figures 9(a) to 9(c). A dip in the reflected spectrum at the high-wavelength end of the spectrum (which is just discernable in figure 7) moves to lower wavelengths as the disbond propagates. The dip in the spectrum

is due to the enhanced local strain in the adherend containing the embedded sensor as a consequence of the disbonding. The intensity of the reflected spectrum of a chirped grating is related to the local density of the grating period; hence, a decrease in the density of the grating period local to the disbond front (due to a local *increase* in the grating spacing because of the enhanced local strain in the adherend) leads to a local decrease in reflected intensity, and consequently a dip in the spectrum. The density of spacings corresponding to positions in the sensor behind the disbond front is increased, so that there is a slight increase of reflected intensity at these higher wavelengths. Figure 10 shows a superposition of the reflected spectra of figures 9(a) to (c), showing the dip in the spectrum moving to shorter reflected wavelengths as the disbond propagates.

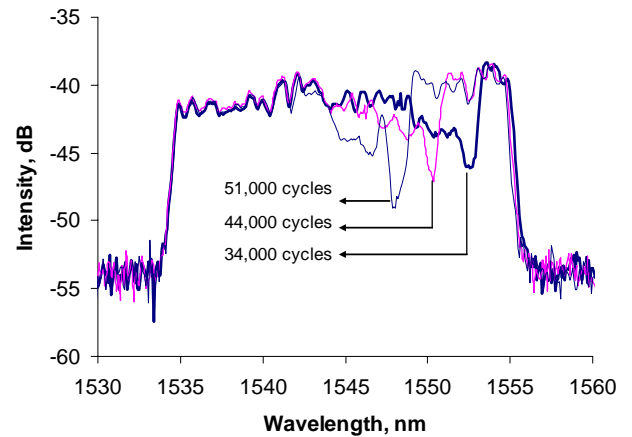


Fig. 10. Superposition of the reflected spectra after 34,000, 44,000 and 51,000 cycles showing the movement of the dip in the spectrum to lower wavelengths as the disbond length increases.

4. Modelling and prediction of the reflected spectra

As in our previous work [16], the issue arises as to the position of the disbond front in relation to the perturbation in the reflected spectrum. The longitudinal strain at the position of the optical fibre sensor has been evaluated using an extension of a 2D analysis used in previous work [16]; with the aid of this strain profile, reflection spectra have been predicted using commercially available OptiGrating software for comparison with the experimental results. The optical fibre has not been modelled explicitly in this work, but the strains have been extracted from the FE model at the location of the

fibre (further details of the modelling can be found in [16]).

The longitudinal strain, (E11) at the position of the centre line of the optical fibre and parallel to the length of the optical fibre was extracted from the FE results and is shown in figure 11 both before disbonding occurs and for a disbond with a length of 10 mm for an applied load of 5 kN. In Figure 11, the distance along the joint is measured from the low-wavelength end of the CFBG sensor which is adjacent to the cut end of the adherend, with the disbond occurring at the other end of the bond overlap length. For the “no disbond” case, the strain in the adherend at the position of the sensor increases as load is transferred from the second adherend, increasing to a plateau region about 5 mm from the end of the adherend. At the other end of the overlap length, the strain in the adherend increases as the load is shed from the termination of the second adherend. Figure 11 also shows the E11 strain for the case of a disbond of length 10 mm adjacent to the high-wavelength end of the CFBG sensor; again, the complexity of the strain field is due to the interaction between the flexure of the joint, the disbond strain field and the load transfer strain field. However, it is the rapid change in strain due to the load-transfer between the adherends which is the most important feature of the strain distribution with regard to the reflected CFBG spectrum.

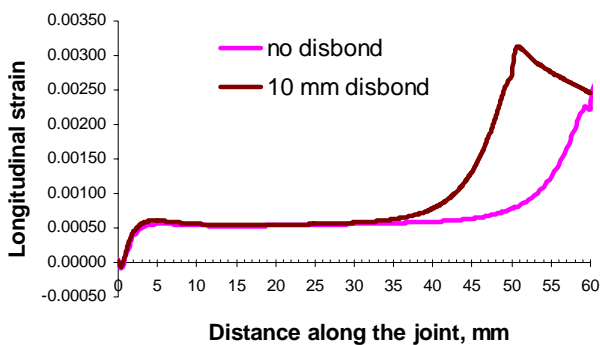


Fig. 11. Strain distribution at the centreline of the optical fibre sensor for the cases of (a) no disbond, and (b) 10 mm disbond.

OptiGrating software [18] has been used to predict the reflected spectrum for a disbond of length 10 mm in order to determine the position of the disbond front in relation to the shape of the reflected spectrum. The CFBG reflection spectrum has been predicted following the method of Okabe,

Takeda and colleagues [12] which modifies the refractive index and grating period as a consequence of the strain profile in order to predict the spectrum using the OptiGrating software. The parameters used in the prediction are: uniform apodization, Poisson’s ratio of 0.17 and photo-elastic coefficients $p_{11} = 0.121$ and $p_{12} = 0.27$, with an index modulation, Δn , of 0.0003.

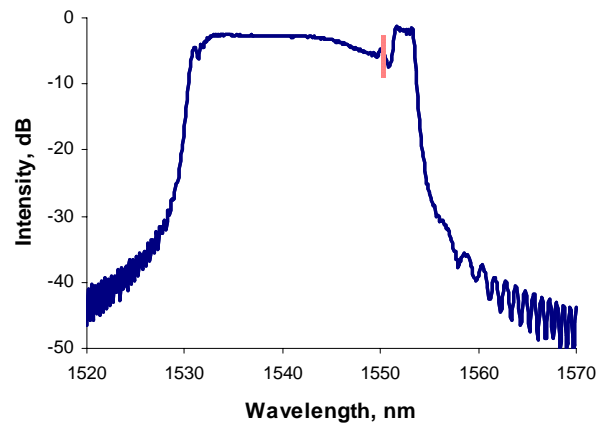


Fig. 12. Predicted reflected spectrum for a 10 mm disbond at the higher wavelength end. The position of the disbond front is indicated by the short vertical line

Figure 12 shows the predicted reflected spectrum which has a sharp dip at the higher wavelength end and which is very similar in shape to the experimental results (see e.g figure 9(a)). In figure 12, the position of the disbond front in relation to the reflected spectrum is shown by a small vertical line. It can be seen that the position of the disbond front corresponds to the beginning of the dip in the reflection spectrum i.e. the position of the disbond front is not at the minimum of the perturbation but about 1.5 mm towards the low-wavelength end of the sensor. This correction has been used to locate the position of the disbond front from the CFBG spectra. Figure 13 compares the position of the disbond front obtained from the CFBG reflection spectra compared with measurements of the disbond front position obtained directly from photographs, for two specimens. There is a good correlation between these measurements, which suggests that the disbond front position can be measured to within about 2 mm.

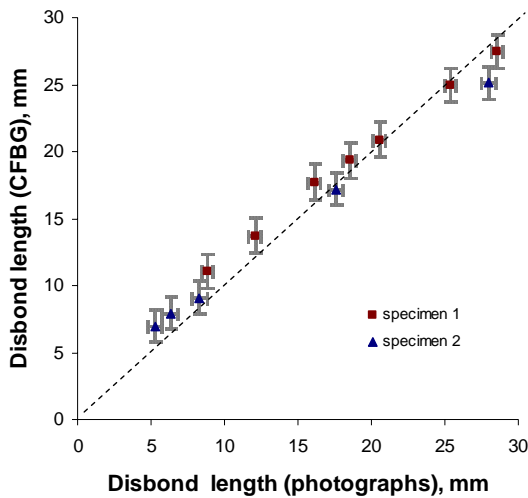


Fig. 13. Comparison of the disbond length obtained using the CFBG sensor with the disbond length measured directly from photographs of the transparent joint.

5 Conclusions

In this paper it has been shown that a chirped fibre Bragg grating sensor can be used to monitor disbonding at either end of an adhesively bonded single-lap joint, with the sensor embedded within one adherend and not within the bondline. Disbond initiation in the bondline adjacent to either the low-wavelength or high-wavelength end of the sensor is indicated by a shift in the spectrum to lower wavelengths (for disbonding at the low-wavelength end) or to higher wavelengths (for disbonding at the high-wavelength end). Disbond propagation is indicated by the movement of a perturbation in the reflected spectrum which corresponds to the progression of the disbond front: for disbonding from the low-wavelength end, the perturbation moves towards higher wavelengths, and for disbonding at the high-wavelength end it moves to lower wavelengths with disbond growth. The detailed shape of the perturbation depends upon the sensor length and reflected bandwidth, but in all cases a combination of finite-element modelling and commercial FBG software enables the position of the disbond front to be related to the perturbation in the reflected spectrum. In general, the position of the disbond front can be located to an accuracy of about 2 mm (this will depend both on adherend materials and sensor position).

Acknowledgement

JP would like to thank the University of Surrey for the provision of a University Research Scholarship.

References

- [1] Cawley P. "Ultrasonic measurements for the quantitative NDE of adhesive joints - potential and challenges". *Ultrasonic symposium. Proc. IEEE*, Tucson, USA, pp 767-772, 1992.
- [2] Lowe M.J.S. , Challis R.E. and Chan C.W. "The transmission of Lamb waves across adhesively bonded lap joints". *J. Acous. Soc. Am.*, Vol 107, No. 3, pp 1333-1345, 2000.
- [3] Meola C., Bruzzone A., Giorleo L., Morace R.E. and Vitiello A. "Application of lock-in thermography in nondestructive evaluation of adhesively-bonded aluminum joints". *J. Adhesion Sci. and Tech.*, Vol 18, No. 6, pp 635-654, 2004.
- [4] Crocombe A.D., Ong C.Y., Chan C.M., Wahab M.A. and Ashcroft I.A. "Investigating fatigue damage evolution in adhesively bonded structures using backface strain measurement". *J. Adhesion.*, Vol. 78, No. 9, pp 745-778, 2002.
- [5] Kuang K.S.C. and Cantwell W.J. "Use of conventional optical fibers and fiber Bragg gratings for damage detection in advanced composite structures: A review". *Appl. Mech. Rev.*, Vol. 56, No.5, pp 493-513, 2003.
- [6] Merzbachery C.I., Kersey A.D. and Friebele E.J. "Fiber optic sensors in concrete structures: A Review". *Smart Mater. Struct.*, Vol .5, No.2, pp 196-208, 1996.
- [7] Takeda S., Aoki Y., Ishikawa T. and Takeda N. and Kikukawa H., "Structural health monitoring of composite wing structure during durability test". *Compos. Struct.*, Vol. 79, pp 133-139, 2007.
- [8] McKenzie .I, Jones R., Marshall I.H. and Galea S. "Optical fibre sensors for health monitoring of bonded repair systems". *Compos. Struct.*, Vol. 50, No. 4, pp 405-416, 2000.
- [9] Herszberg I., Li H.C.H., Dharmawan F., Mouritz A.P., Nguyen M. and Bayandor J. "Damage assessment and monitoring of composite ship joints". *Compos. Struct.*, Vol. 67, No. 2, pp 205-216, 2005.
- [10] Jones R. and Galea S. "Health monitoring of composite repairs and joints using optical fibres". *Compos. Struct.*, Vol. 58, No.3, pp 397-403, 2002.
- [11] Palaniappan J., Wang H., Ogini S.L., Thorne A.M., Reed G.T., Tjin S.C. and McCartney L.N. "Prediction of the reflected spectra from chirped fibre Bragg gratings embedded within cracked crossply laminates". *Meas. Sci. Technol.* Vol 17, No. 6, pp 1609-1614, 2006
- [12] Takeda S., Okabe Y. and Takeda N. "Application of chirped FBG sensors for detection of local

- delamination in composite laminates". *Proc. SPIE*, Vol. 5050, pp 171-178, 2003.
- [13] Minakuchi S., Okabe Y. and Takeda N. "Real-time detection of debonding between honeycomb core and facesheet using a small-diameter FBG sensor embedded in adhesive layer". *J. Sandwich Struct. Mater.* Vol. 9, No. 1, pp 9–33, 2007
- [14] Capell T.F., Palaniappan J., Ogin S.L., Crocombe A.D., Reed G.T., Thorne A.M., Mohanty L. and Tjin S.C. "The use of an embedded chirped fibre Bragg grating sensor to monitor disbond initiation and growth in adhesively bonded composite/metal single lap joints". *J. Opt. A: Pure Appl. Opt.*, In Press, 2007
- [15] Palaniappan J., Wang H., Ogin S.L., Thorne A.M., Reed G.T., Crocombe A.D. and Tjin S.C. "Structural health monitoring of bonded composite joints using embedded chirped fibre Bragg gratings". *Adv. Comp. Letters*, Vol. 14, No.6, pp 185-192, 2005.
- [16] Palaniappan J., Wang H., Ogin S.L., Thorne A.M., Reed G.T., Crocombe A.D. and Tjin S.C. "Changes in the reflected spectra of embedded chirped fibre Bragg gratings used to monitor disbonding in bonded composite joints" . *Compos. Sci. Technol.* available online. 2007.
- [17] Okabe Y., Tsuji R. and Takeda N. "Application of chirped fiber Bragg grating sensors for identification of crack locations in composites". *Compos. Part A: Appl. Sci. and Manuf.*, Vol 35, No 1, pp 59-65, 2004
- [18] OptiGrating, Integrated and Fiber Optical Gratings Design Software (version 4.2), Optiwave Corporation, Canada